

A Switch Between Cytoprotective and Cytotoxic Autophagy in the Radiosensitization of Breast Tumor Cells by Chloroquine and Vitamin D

Eden N. Wilson · Molly L. Bristol · Xu Di · William A. Maltese · Kristen Koterba · Matthew J. Beckman · David A. Gewirtz

Published online: 2 September 2011
© Springer Science+Business Media, LLC 2011

Abstract Calcitriol or 1,25-dihydroxyvitamin D₃, the hormonally active form of vitamin D, as well as vitamin D analogs, has been shown to increase sensitivity to ionizing radiation in breast tumor cells. The current studies indicate that the combination of 1,25-dihydroxyvitamin D₃ with radiation appears to kill p53 wild-type, estrogen receptor-positive ZR-75-1 breast tumor cells through autophagy. Minimal apoptosis was observed based on cell morphology by DAPI and TUNEL staining, annexin/PI analysis, caspase-3, and PARP cleavage as well as cell cycle analysis. Induction of autophagy was indicated by increased acridine orange staining, RFP-LC3 redistribution, and detection of autophagic vesicles by electron microscopy, while autophagic flux was monitored based on p62 degradation. The autophagy inhibitors, chloroquine and bafilomycin A1, as well as genetic suppression of the autophagic signaling proteins Atg5 or Atg 7 attenuated the impact of the combination treatment of 1,25 D₃ with radiation. In contrast to autophagy mediating the effects of the combination treatment, the autophagy induced by radiation alone was apparently cytoprotective in that either

pharmacological or genetic inhibition increased sensitivity to radiation. These studies support the potential utility of vitamin D for improving the impact of radiation for breast cancer therapy, support the feasibility of combining chloroquine with radiation for the treatment of breast cancer, and demonstrate the existence of an “autophagic switch” from cytoprotective autophagy with radiation alone to cytotoxic autophagy with the 1,25 D₃–radiation combination.

Keywords Breast cancer · Vitamin D · Radiation · Autophagy · Chloroquine

Abbreviations

1,25 D ₃	1,25 dihydroxyvitamin D ₃
DAPI	4',6-diamidino-2-phenylindole
AO	Acridine orange
AVOs	Acidic vacuolar organelles
CQ	Chloroquine
IR	Ionizing radiation
TUNEL	Terminal deoxynucleotidyl transferase dUTP nick end labeling
TEM	Transmission electron microscopy
BAF	Bafilomycin A1
SS	Serum starvation
PI	Propidium iodide
FACS	Fluorescence-activated cell sorting

Electronic supplementary material The online version of this article (doi:10.1007/s12672-011-0081-7) contains supplementary material, which is available to authorized users.

E. N. Wilson · M. L. Bristol · X. Di · M. J. Beckman · D. A. Gewirtz (✉)
Department of Pharmacology and Toxicology,
Massey Cancer Center, Virginia Commonwealth University,
PO Box 980035, Richmond, VA 23298, USA
e-mail: gewirtz@vcu.edu

W. A. Maltese · K. Koterba
Department of Biochemistry and Cancer Biology,
University of Toledo College of Medicine,
Toledo, OH 43614, USA

Introduction

Radiation therapy is a widely used component of cancer therapy and is a fundamental tool in the treatment of breast cancer (along with surgery and chemotherapy). Exposure to ionizing radiation (IR) leads to rapid generation of reactive

oxygen species that produce DNA damage [1]. One of the most lethal radiation-induced lesions in DNA is the double-strand break [2], which can lead to growth arrest or cell death by the activation of various signaling pathways. Although radiation is a very effective modality in the treatment of breast cancer, there is always some likelihood of disease recurrence that may be due to tumor cells that survive through disruptions in cell death pathways, increased DNA repair capacity, and/or overactivation of cytoprotective signaling pathways [3]. Thus, a primary goal of our work has been to develop strategies to enhance the response to radiation therapy using the active form of vitamin D, calcitriol (1,25 D3) as well as analogs of vitamin D [4, 5]. Apart from the established role of vitamin D3 in regulation of calcium homeostasis, numerous studies have shown that the metabolically active form of vitamin D3, 1,25-dihydroxyvitamin D3, (1,25 D3) as well as vitamin D analogs can enhance the response to chemotherapy in a variety of malignancy models [6–9].

Autophagy is an evolutionary conserved process where-by cytoplasmic proteins and cellular organelles are enveloped in autophagosomes and degraded by fusion with lysosomes for amino acid and energy recycling [10]. There is evidence that whereas autophagy can play a critical role in cellular survival [11–14], it can also become a cellular suicide pathway when apoptosis is defective and following extreme stress conditions [15–17]. Furthermore, autophagy is frequently activated in tumor cells following anticancer therapies such as drug treatment and gamma irradiation [18] and can either contribute to cell death or represent a mechanism of resistance to these treatments [11, 12, 14, 19–23].

A number of studies have demonstrated that radiation induces cytoprotective autophagy [12, 16, 22, 23]. However, studies from our laboratory have indicated that autophagy is the basis for radiation sensitization of MCF-7 breast tumor cells by 1,25 D3 [5]. Studies by other investigators have also demonstrated radiation sensitization through the promotion of autophagy [24–26].

Autophagic cell death has been defined based on characteristics such as (1) cell death occurring without the involvement of apoptosis and necrosis; (2) increased autophagic flux, rather than an increase of autophagic markers; and (3) suppression of autophagy via both pharmacological inhibitors and genetic approaches is able to rescue or prevent cell death [27]. In the present manuscript, we have established that autophagic cell death is the mode of radiosensitization by 1,25 D3 in ZR-75-1 breast tumor cells. We were further able to demonstrate that autophagy can actually have dual functions in the same experimental system, acting both as a cytoprotective mechanism for radiation alone and a cytotoxic mechanism when radiation is accompanied by 1,25 D3.

Results

Sensitization to Ionizing Radiation by 1,25 D3 in ZR-75-1 Breast Tumor Cells

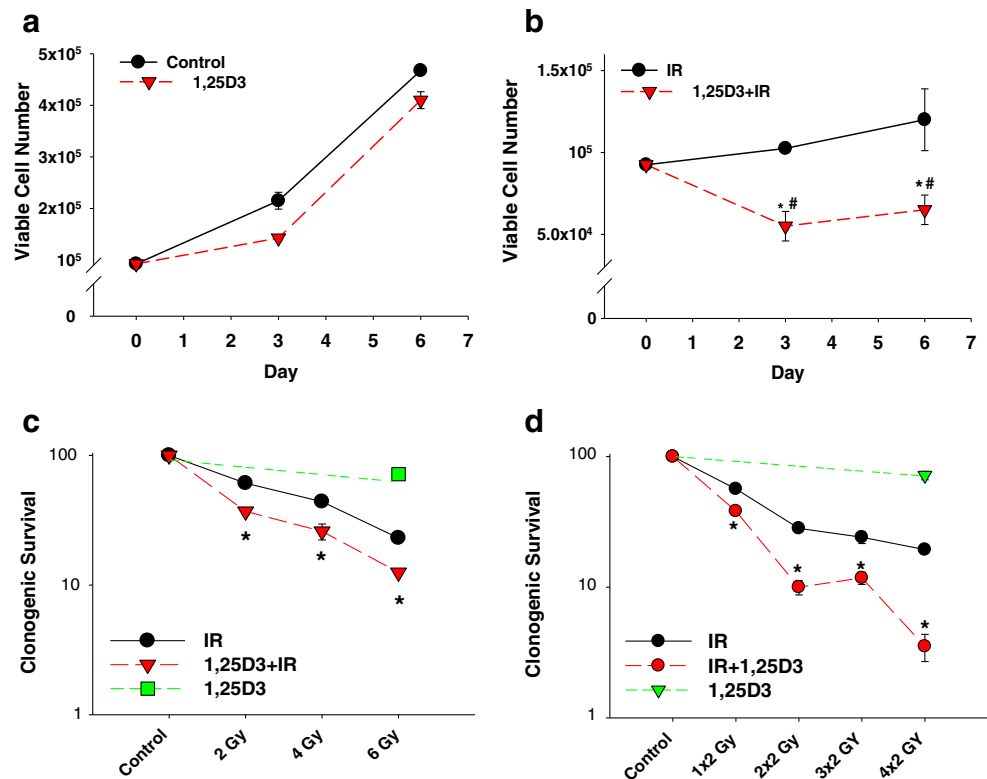
Initial studies assessed the influence of treatment with 1,25 D3 on sensitivity to radiation. Exposure of ZR-75-1 cells to 1,25 D3 alone had a modest impact on cell growth; at day 3, control cells had doubled approximately 2.5 times, whereas cells treated with 1,25 D3 had doubled approximately two times (Fig 1a). This is likely due to 1,25 D3's regulation of proteins involved in cell cycle progression [28, 29]. Figure 1b shows that the combination of 1,25 D3 with radiation resulted in a reduction of viable cells (actual cell killing) that was followed by growth arrest in the residual surviving cell population; in contrast, radiation alone appeared to inhibit cell growth without producing an actual reduction in viable cell number (compared to control growth in Fig. 1a).

Radiosensitization of ZR-75-1 breast cancer cells by 1,25 D3 was further assessed in clonogenic survival assays using both single dose (Fig. 1c) and fractionated dose radiation (Fig. 1d). When combined with 1,25 D3, there was a pronounced decrease in clonogenicity compared to radiation alone at all doses. As in the studies presented in Fig. 1a, 1,25 D3 alone had a minimal impact on clonogenicity, indicating that the sensitization to radiation is likely not simply a result of additive toxicity.

Minimal Induction of Apoptosis by Radiation and 1,25 D3±IR

Figure 2 presents studies that were designed to assess whether apoptosis was the basis for the radiosensitization by 1,25 D3. Apoptosis was assessed by the terminal deoxynucleotidyl transferase dUTP nick end labeling (TUNEL) assay and 4',6-diamidino-2-phenylindole (DAPI) staining (Fig. 2a), fluorescence-activated cell sorting (FACS) analysis for annexin/propidium iodide (PI) staining (Fig. 2b), Western blot analysis for both PARP and caspase-3 cleavage (Fig. 2c), and FACS analysis for a sub-G1 population (Fig. 2d). The TUNEL and DAPI staining data indicate that minimal apoptosis occurs with either radiation alone or 1,25 D3+radiation. This result was confirmed by annexin V/PI staining where there is minimal staining in quadrants Q2 and Q4, which are indicative of early and late apoptotic cells; there was also no evidence of necrosis (quadrant Q1). Furthermore, with both radiation alone and 1,25 D3+radiation, there is no indication of an increase in the sub-G1 population (Fig. 2d). Cell cycle analysis also indicates that there is no mitotic catastrophe, due to the lack of accumulation of cells with DNA content greater than 4n [30, 31]. Staurosporine was used as a positive control to demonstrate that ZR-75-1 cells have the ability to undergo apoptosis (Fig. 2a, b).

Fig. 1 Sensitization to ionizing radiation by 1,25 D3. **a–b** Viable cell number was determined by exclusion of trypan blue at days 3 and 6 post-initial treatment. **a** Cells were exposed to 100 nM 1,25 D3 continuously. **b** Cells received fractionated doses of 4×2 Gy (over a period of 2 days) or were treated concurrently with 1,25 D3 and 4×2 Gy radiation. **c–d** Clonogenic survival assays with both single dose and fractionated radiation, with or without 100 nM 1,25 D3. Clonogenic survival was assessed after 14 days. Values shown are from a representative experiment with triplicate samples for each condition. * $p < .05$ compared to control # $p < .05$ compared to IR alone **(b)** * $p < .05$ compared to IR **(c–d)**. Data are representative of an average of three experiments



Autophagy Induction and Autophagic Flux by Radiation Alone and 1,25 D3+IR

Autophagy has been shown to play an important role in cell survival and cell death [32, 33]. To investigate whether autophagy plays a role in radiation sensitization in the ZR-75-1 cells, cells were stained with acridine orange (AO), and the formation of punctate staining was monitored based on visual assessment (Fig. 3a) as well as quantification using flow cytometry (Fig. 3b, c). Figure 3b presents a representative set of histograms for each treatment, while Fig. 3c summarizes data from two replicate experiments. At 72 h post-irradiation, there is an approximately fourfold increase in the percent of acidic vacuolar organelles (AVOs) in cells that received radiation treatment alone and an approximately fivefold increase by the combination treatment; the increase produced by 1,25 D3 alone did not achieve statistical significance (Fig. 3c). Time course data suggest that autophagy is initiated earlier in cells treated with 1,25 D3+IR, and autophagy is sustained to a higher extent with 1,25 D3+IR treatment compared to radiation treatment alone (Online Resource 1(S1)). The promotion of autophagy by both radiation alone and 1,25 D3+radiation was confirmed by monodansylcadaverine (MDC) [34] staining (Online Resource 1(S2)) and red fluorescent protein-light chain 3 (RFP-LC3) redistribution (Fig. 3d). Upon autophagy induction, RFP-LC3 displays punctate staining in the cytoplasm and can be visualized using confocal microscopy [35]. Quantification of RFP-LC3

puncta is presented in Fig. 3e. Consistent with AO staining, there is essentially the same number of LC3 puncta per cell for IR and 1,25 D3+IR treatment at 72 h. Transmission electron microscopy (TEM) images also indicate the presence of autophagosomes with the combination treatment as well as with radiation alone (Fig. 3f).

Since the presence of autophagic vesicles does not necessarily mean that the autophagosomes have fused with the lysosome and that the contents of the autophagosome have been degraded, autophagic flux was assessed by Western blot analysis for p62 degradation. p62 binds directly to LC-3 (Atg8), a critical protein involved in autophagosome formation to facilitate autophagic degradation [36–38]. Consistent with the AO staining and electron microscopy data, there was no p62 degradation with 1,25 D3 alone (Online Resource 1(S3)), while p62 degradation is shown with serum starvation (SS), which was used as a positive control. In the case of both radiation alone and 1,25 D3+radiation, p62 degradation appears to be virtually complete within 72 h (Fig. 3g).

Residual Surviving Cells Are in a State of Senescence

In previous studies, we reported that MCF-7 cells undergo a period of growth arrest/senescence following treatment with radiation alone as well as in the residual surviving breast tumor cell population following treatment with vitamin D analog, EB1089+radiation [4]. Based on cell morphology and β -galactosidase staining, residual surviving cells are

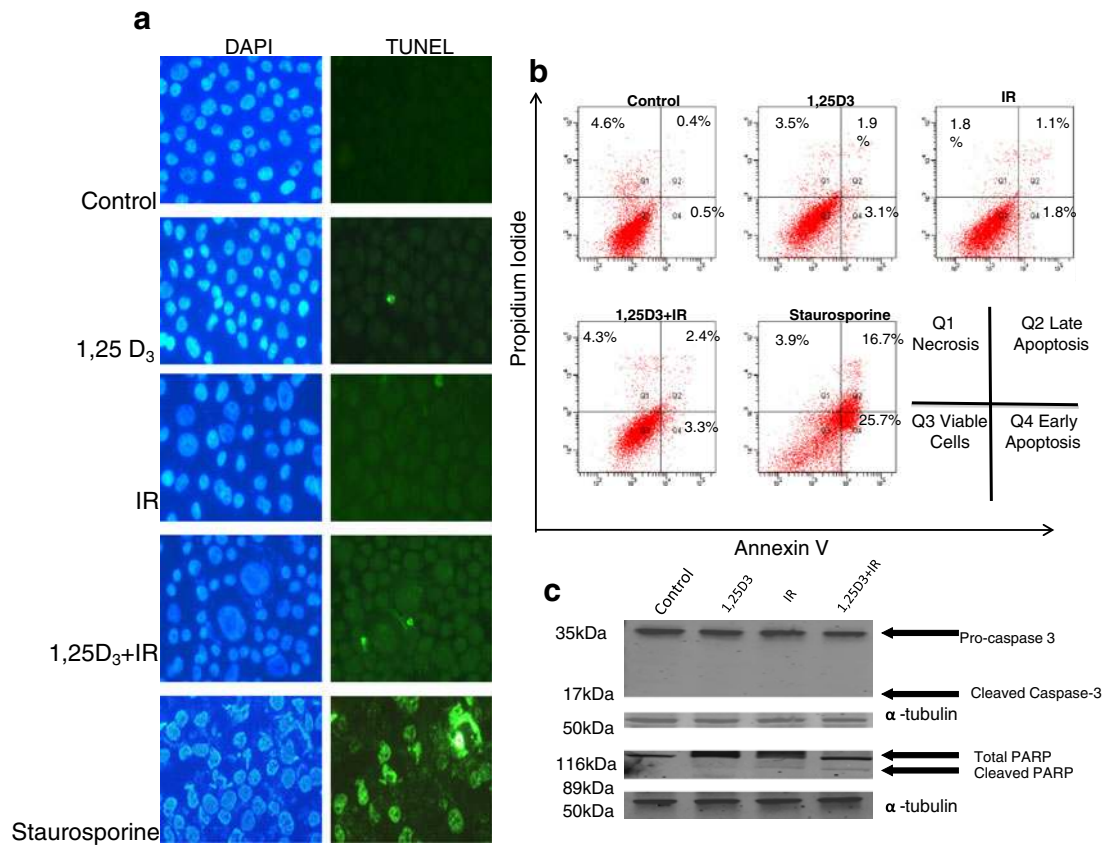


Fig. 2 Minimal induction of apoptosis by radiation and 1,25 D3±IR. Cells were treated with 100 nM 1,25 D3 alone, fractionated doses of radiation (4×2 Gy), or 1,25 D3 concurrently with radiation. **a** TUNEL assay and DAPI-stained images were taken 72 h post-initial drug treatment. **b** Annexin V- and PI-positive cells were analyzed by FACS. Exposure to 500 nM staurosporine for 24 h was used as a positive control. **c** Western blotting for cleavage of caspase-3 and PARP 72 h post-initial treatment. Alpha tubulin was used as a loading control. **d** Cell cycle distribution by flow cytometry 72 h post-initial treatment. Data are representative of an average of three experiments

indeed in a state of senescence after both radiation alone and 1,25 D3+radiation treatment (Fig. 4a). To further confirm β -galactosidase activity, 5-dodecanoylamino fluorescein di- β -D-

galactopyranoside (C12FDG), a fluorogenic substrate for β -gal activity [39], was analyzed by FACS analysis, and fluorescence intensity was measured (Fig. 4b and Online Resource 2(S4)). For both experimental conditions, senescence is most pronounced at 144 h posttreatment.

Effects of Pharmacologic Autophagy Inhibition on Cell Viability After IR and 1,25 D3±IR

In efforts to confirm that autophagy is the basis for sensitization by 1,25 D3, studies were conducted with the autophagy inhibitors chloroquine (CQ) and bafilomycin A1

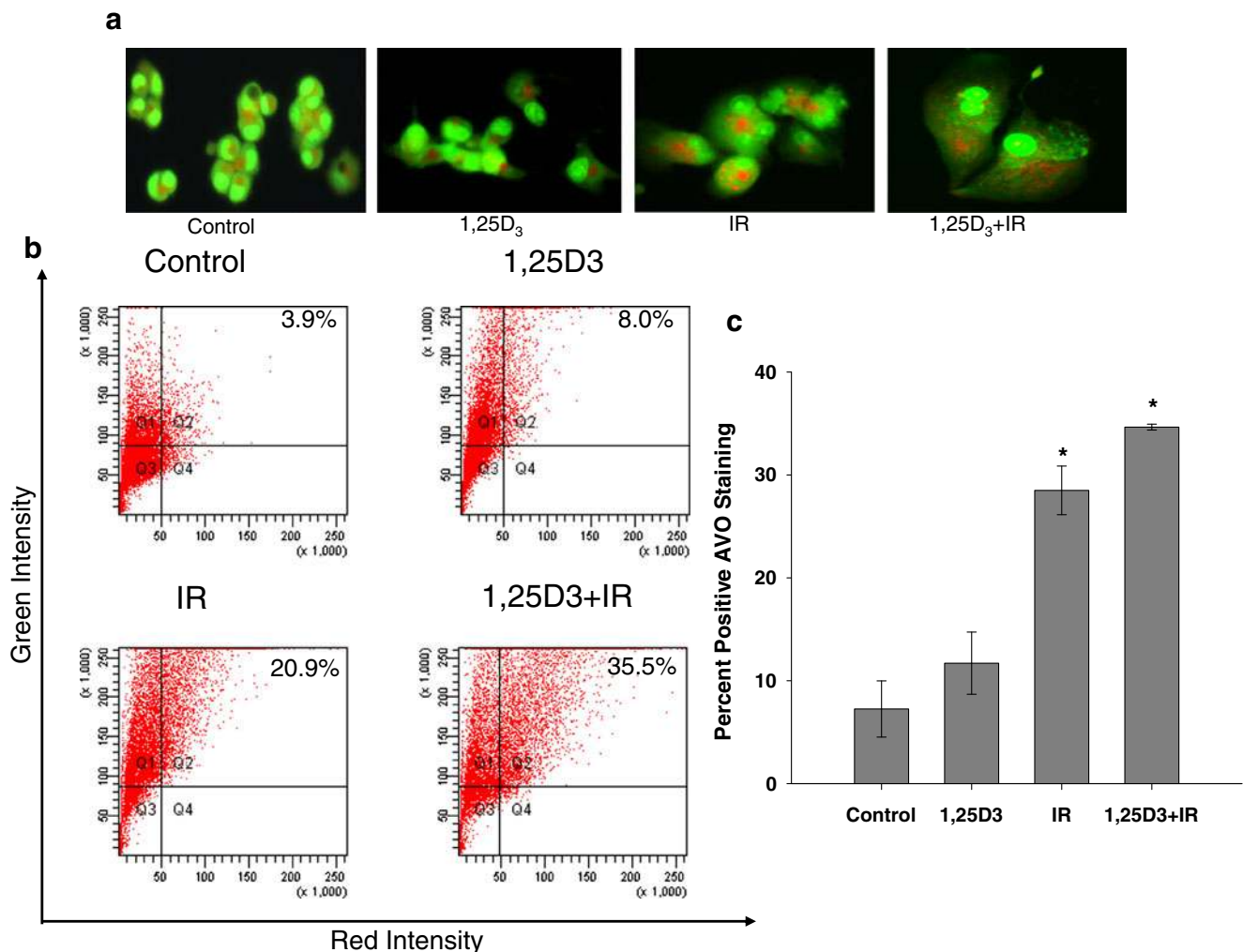


Fig. 3 Autophagy induction and autophagic flux after IR and 1,25 D3±IR. Cells were exposed to 100 nM 1,25 D3 alone, radiation alone (4×2 Gy) administered over a period of 2 days, or 1,25 D3 concurrently with radiation. **a** Acridine orange images were taken at 72 h post-initial treatment (1,25 D3,IR, or 1,25 D3+IR) using an inverted fluorescent microscope. Cells with positive staining for AVOs were monitored using flow cytometry 72 h posttreatment. **b** Representative histograms of positive acridine orange staining for each treatment. **c** Percentage of cells with positive acridine orange staining represented as the mean±SE. **d–e** RFP-LC3 was assessed by

confocal microscopy 72 h posttreatment. **f** The presence of autophagic vacuoles was confirmed by electron microscopy at 72 h. Autophagosomes are indicated by the *red arrows*. **g** Autophagic flux was based on the decline in p62 levels monitored by Western blotting post-irradiation. β -Actin was utilized as a loading control, and SS was used as a positive control for autophagic flux. Values shown are from a representative experiment with triplicate samples for each condition. * $p < 0.05$ compared to control. Data are representative of an average of three experiments

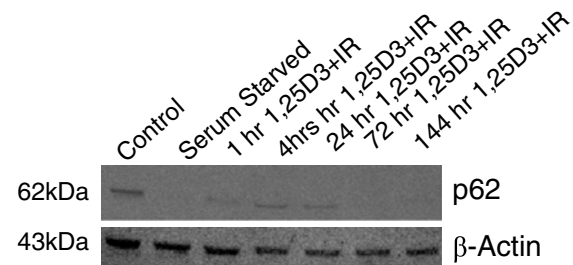
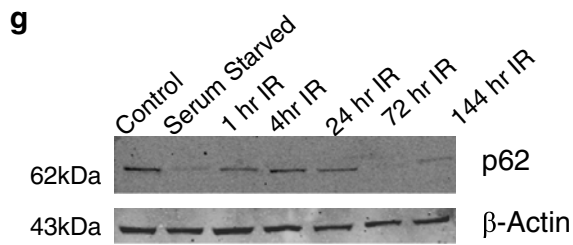
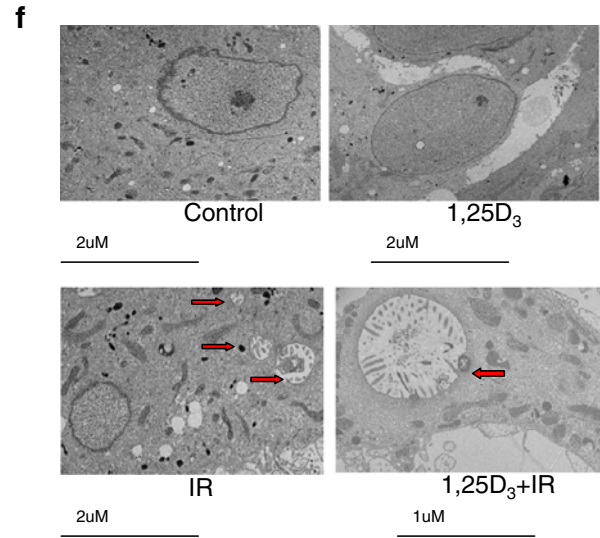
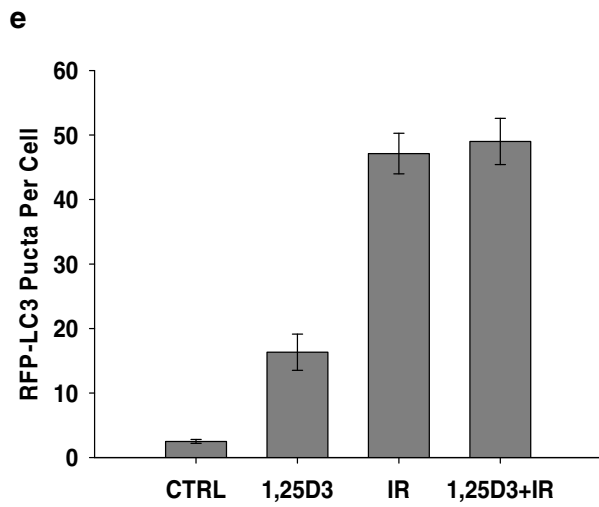
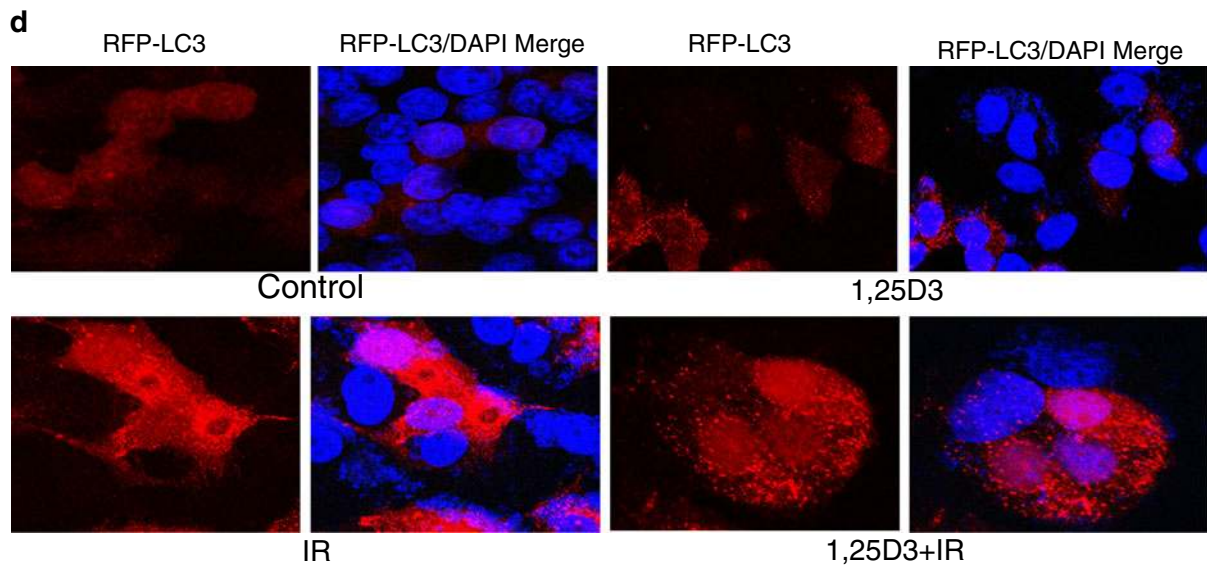


Fig. 3 (continued)

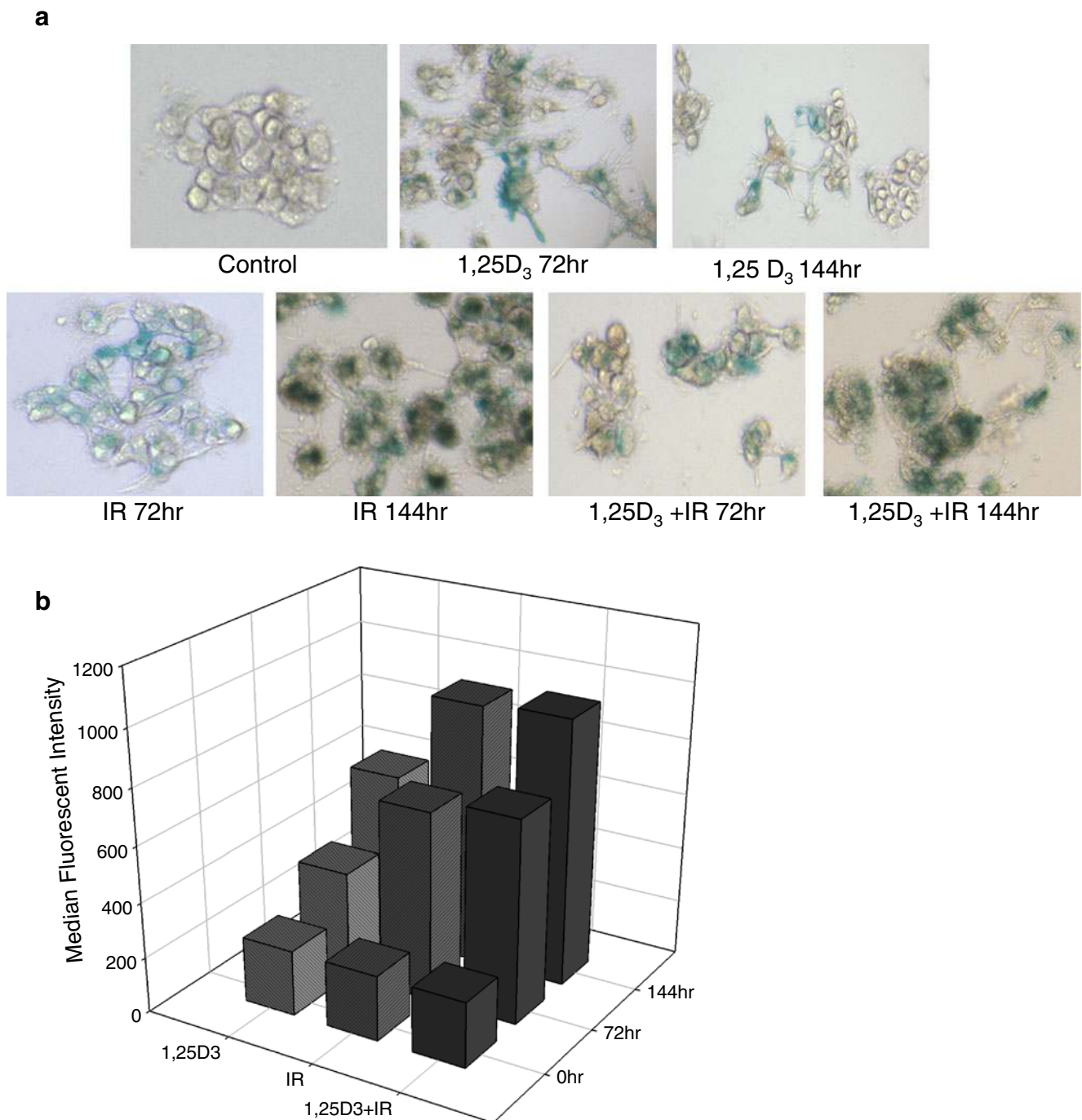


Fig. 4 Residual surviving cells in a state of senescence. Cells were exposed to 100 nM 1,25 D₃, radiation (4×2 Gy) administered over a period of 2 days, or 1,25 D₃ concurrently with radiation. Cells were stained with β-galactosidase, and images were taken at 3 and 6 days post-initial drug treatment or post-irradiation. **a** Data are representative

(BAF). BAF prevents the fusion of the autophagosome with the lysosome [33, 40], while CQ prevents the acidification of the lysosome [41]. We identified concentrations of BAF and CQ that would have little to no toxic effects, as indicated by trypan blue exclusion as well as the MTT assay (Online Resource 3(S5–S6)). Inhibition of the autophagy induced by

images from three experiments. **b** Cells were exposed to 1,25 D₃, radiation alone, or 1,25 D₃+IR, and samples were stained as described in “Materials and Methods” Section and analyzed by FACS analysis at days 3 and 6 posttreatment. Values shown are from a representative experiment with triplicate samples for each condition

either radiation or 1,25 D₃+radiation (specifically the formation of acidified autophagic vesicles) was confirmed through an assessment of AO distribution by flow cytometry (Fig. 5a and Online Resource 3 (S7)).

Treatment with radiation concurrently with BAF or CQ resulted in a significant enhancement of cytotoxicity as

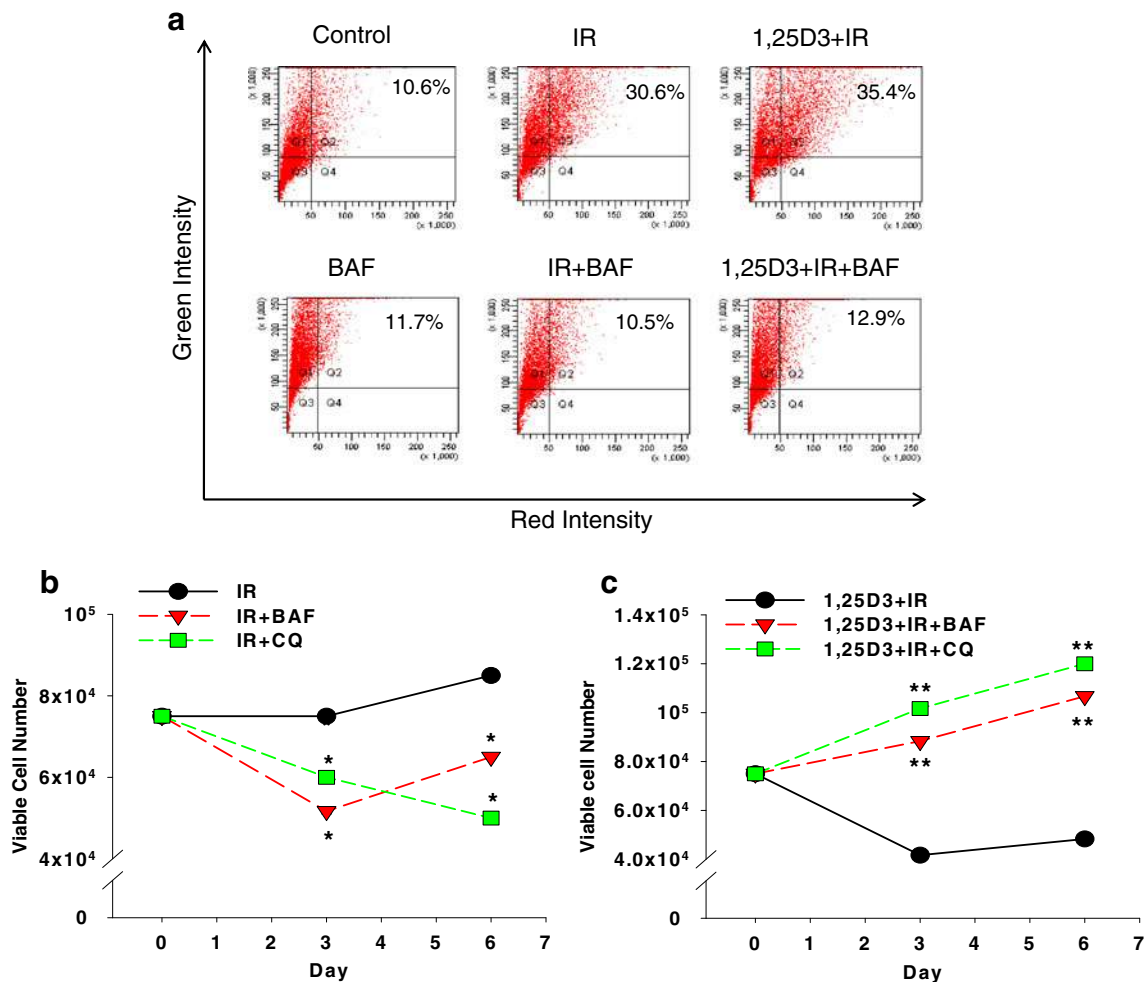


Fig. 5 Effects of pharmacologic autophagy inhibition on cell viability in IR and 1,25 D3±IR-treated cells. **a** Cells were exposed to 4×2 Gy radiation alone or concurrently with BAF or CQ, and percentage of cells with positive AVO staining was monitored using flow cytometry at 72 h posttreatment. **b** Cells were exposed to radiation in the absence or presence of either BAF or CQ, and viable cell number was assessed by trypan blue exclusion at days 3 and 6 posttreatment. **c** Cells were

exposed to 1,25 D3 concurrently with 4×2 Gy radiation in the absence or presence of either BAF or CQ, and viable cell number was assessed by trypan blue exclusion at days 3 and 6 posttreatment. Values shown are from a representative experiment with triplicate samples for each condition. * $p < .05$ compared to IR (**b**) ** $p < .05$ compared to 1,25 D3+IR (**c**). Data are representative of an average of three experiments

indicated by the decline in viable cell number (Fig. 5b). These observations are consistent with the premise that autophagy induced by radiation alone is cytoprotective. In dramatic contrast, interference with autophagy in 1,25 D3+IR-treated cells results in reduced radiation sensitivity, which is the expected outcome if autophagy mediates the cytotoxicity of the 1,25 D3–radiation combination treatment. In fact, the cell death induced by the combination treatment is attenuated, and cell viability is restored to levels similar to what is observed with IR treatment alone (comparing Fig. 5b and c). These results were confirmed by monitoring propidium iodide uptake by flow cytometry. Radiosensitization by CQ appears to be a result of the promotion of both apoptosis and necrosis (Online Resource 3 (S8–S9)). Moreover, these findings indicate the existence of both cytoprotective and cytotoxic func-

tions of autophagy in response to radiation in the same experimental system.

Effects of Genetic Autophagy Inhibition on Cell Viability in IR and 1,25 D3±IR-Treated Cells

To confirm the results generated with pharmacological autophagy inhibition, additional studies were performed using ZR-75-1 cells in which expression of either ATG-5 or ATG-7 was stably suppressed by shRNA. Atg5 combines with Atg12 in a multimeric protein complex that is required for autophagosome formation, whereas Atg7 is an E1-like enzyme involved in activating both LC3II (Atg8) and Atg5 [42]. Atg5 levels were reduced by approximately 77% and Atg7 levels by approximately 60% (Fig. 6a). To determine if this knockdown was sufficient to alter autophagic

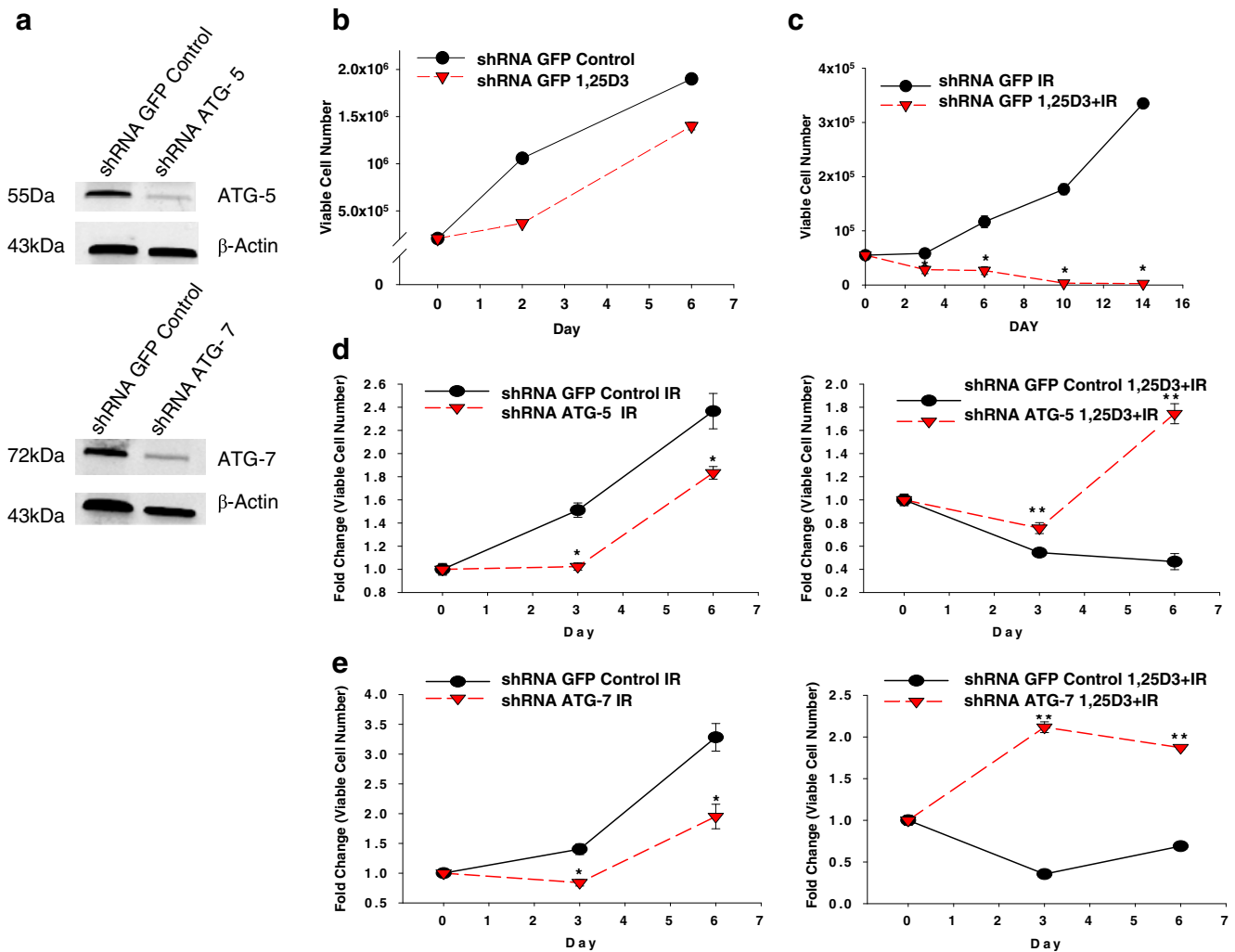


Fig. 6 Effects of genetic autophagy inhibition on cell viability in IR and 1,25 D3+IR-treated cells. **a** ZR-75-1 cells were stably transfected with either a lentivirus encoding shRNA against GFP (control) or with a lentivirus for silencing expression of ATG-5 or ATG-7. Atg5 levels are shown by Western blotting comparing control cells to those with ATG-5 or ATG-7 knockdown. Beta-actin was used as loading control. **b–c** shRNA control cells were treated continuously with 1,25 D3 (**b**), a single dose of 4 Gy or concurrently with 1,25 D3 and IR (**c**), and cell

viability was assessed by trypan blue exclusion. **d–e** Cell viability was assessed by trypan blue exclusion in cells receiving a single dose of 4 Gy IR or 1,25 D3+IR in ATG-5-silenced cells (**d**) or ATG-7-silenced cells (**e**). Values shown are from a representative experiment with triplicate samples for each condition. * $p < .05$ compared to IR, ** $p < 0.05$ compared to 1,25 D3+IR. Data are representative of an average of three experiments

function, autophagic flux was monitored by p62 degradation in ATG-5 and ATG-7 knockdown cells. Indeed, cells in which ATG-5 or ATG-7 had been knocked down displayed decreased autophagic flux compared to vector control cells following SS (Online Resource 4 (S10)).

Initial studies were conducted to confirm that 1,25 D3, IR, and 1,25 D3+IR treatment produced the same relative effects in control cells expressing shRNA against GFP (shRNA GFP control) as they did in the parental ZR-75-1 cells. A single dose of 4-Gy radiation was used for these studies as we found that this dose allowed us to more effectively distinguish the effects of radiation alone from the combination treatment in these genetically modified cells. Figure 6b shows transient

growth inhibition by 1,25 D3, while Fig. 6c indicates that indeed 1,25 D3 sensitized shRNA control cells to IR treatment. In the cells where ATG-5 was partially silenced, sensitivity to radiation was increased compared to the shRNA control cells, again indicating that autophagy is a mode of cell protection for radiation alone (Fig. 6d, left panel). In dramatic contrast, the impact of 1,25 D3+radiation is blunted or attenuated when ATG-5 is suppressed, which supports the cytotoxic actions of autophagy for the 1,25 D3 +radiation combination treatment (Fig. 6d, right panel).

The studies in the ATG-7 suppressed cells demonstrated an essentially identical outcome as with the pharmacological inhibitors CQ and BAF as well as with suppression of ATG-5.

That is, sensitivity to radiation alone is increased, albeit quite modestly, (Fig. 6e, left panel) while radiosensitization by 1,25 D3 is markedly attenuated (Fig. 6e, right panel). Knockdown of ATG-5 or ATG-7 had no perceptible effect on the capacity of 1,25 D3 treatment alone to moderately inhibit cell growth (Online Resource 4 (S11) and (S12)).

Discussion

The current studies further establish the potential utility of vitamin D as an adjuvant therapy for the treatment of breast cancer and furthermore provide evidence that sensitization to radiation by 1,25 D3 occurs through the promotion of autophagy. Consequently, the combination treatment is likely to be effective even in breast tumor cells that might be resistant to apoptosis. Interestingly, 1,25 D3 appears to switch the cells from a cytoprotective to a cytotoxic mode of autophagy. Although either cytoprotective or cytotoxic actions of autophagy have been reported in multiple publications, to our knowledge, these are the first studies in the literature to provide evidence for this type of “autophagic switch.”

While 1,25 D3 treatment promotes cell killing in response to radiation in ZR-75-1 breast cancer cells, our studies do not support the involvement of apoptosis in the actions of radiation alone or for the combination treatment. Instead, our data support the promotion of autophagic cell death as the mode of radiation sensitization by 1,25 D3. In confirmation of the conclusion that sensitization to radiation by 1,25 D3 is a consequence of the induction of cytotoxic autophagy, pharmacologic and genetic interference with autophagy resulted in increased cell survival, with viable cell numbers essentially restored to levels observed after treatment with radiation alone. Conversely, when autophagy was blocked in cells irradiated in the absence of 1,25 D3, there was clearly a decrease in cell viability, supporting the induction of cytoprotective autophagy by radiation alone. Our data further suggest that residual surviving cells are in a state of senescence, which is consistent with studies showing that radiation induces senescence in tumor cells [43, 44].

Although the amount of autophagy induced appears to be essentially the same in both IR and 1,25 D3+IR treatment, we speculate that 1,25 D3 increases the rate and extent of autophagic flux in radiation-treated cells and that this increase mediates the radiosensitizing effects of 1,25 D3. This hypothesis is based on the fact that p62 is degraded earlier and to a greater extent in 1,25 D3+IR-treated cells compared to IR treatment alone. It is important to emphasize that this system should provide the appropriate experimental model to address the question of what

factors might distinguish cytoprotective from cytotoxic autophagy, which is currently a fundamental question in this field [27].

Our future studies will be designed to elucidate the pathways by which 1,25 D3 sensitizes breast cancer cells, and establish what factors determine whether autophagy will be cytotoxic or cytoprotective. It is known that autophagy is a multi-step process that appears to be regulated by various signaling pathways [25, 45]. Moreover, activation of ER stress and mTOR signaling pathways have been shown to be involved in autophagy induction [46, 47]. Both pathways have been shown to be activated in response to radiation [48], and studies have shown that AKT/mTOR signaling is involved in 1,25 D3's effects on cell proliferation [49, 50]. The capacity of 1,25 D3 to promote radiosensitization may involve its modulation of proteins in one or both of these autophagy pathways.

Materials and Methods

Cell Lines

The p53 wild-type ZR-75-1 human breast tumor cell line was obtained from ATCC. The ZR-75-1 ATG5 KD and ATG7 KD cells were generated as indicated below.

RNA Interference

The siRNA sequence to target ATG-5 was obtained from a previous publication [51]. The sequence of the siRNA was: GCAACTCTGGATGGGATTG. It was ordered as a hairpin oligonucleotide with the sense and antisense sequence separated by a loop sequence and restriction sites at the 5' and 3' ends to facilitate cloning into System Bioscience's pSIH-H1-puro lentiviral shRNA vector (which uses the H1 promoter to drive expression). With the shRNA inserted into this vector, lentivirus was produced in HEK 293TN cells co-transfected with the following vectors that encode the necessary packaging components: pPack-Rev, pPack-Gag, and pPack-VSVg (purchased from Systems Biosciences as a mix). The virus shed into the medium was then used to infect the ZR-75-1 cells. The latter were selected in medium with 1 µg/mL puromycin to enrich the infected cells. A 70% KD of Atg5 in these cells was observed following selection. shRNA control cells were generated in similar fashion except that the siRNA sequence used was against the irrelevant *Aequorea victoria* green fluorescent protein (GFP).

Mission shRNA lentiviral transduction particles for ATG-7 (Sigma NM_006395) were purchased as a set of five different shRNA viral particles. After infecting the ZR-75-1 target cells with each of the five different viral populations, each at three different MOIs, the cells were

checked for Atg7 expression, and the culture that displayed the greatest decrease in Atg7 expression was selected. The Sigma particles that worked best were #TRCN000007584 (at an MOI of 0.5), with shRNA directed against the following sequence in the 3'UTR of ATG-7: GCCTG CTGAGGAGCTCTCCA. The transduced cells were selected within medium with 1 $\mu\text{g}/\text{mL}$ puromycin to obtain stable cell lines.

Cell Culture and Treatment

All ZR-75-1-derived cell lines were grown from frozen stocks in basal RPMI 1640 supplemented with 5% FCS, 5% BCS, 2 mmol/L L-glutamine, and penicillin/streptomycin (0.5 mL/100 mL medium). ZR-75-1/ATG5 KD and ATG-7 KD cells were maintained using (1 $\mu\text{g}/\text{mL}$) puromycin (Sigma p8833) for resistance. All cells were maintained at 37°C under a humidified 5% CO₂ atmosphere. Cells were exposed to γ -IR using a ¹³⁷Cs irradiator. In our studies, cells were exposed to 100 nmol/L 1,25 vitamin D₃ (Sigma D1530) alone or concurrently with radiation treatment. In the cases where the radiation doses were fractionated, four fractions of 2-Gy radiation were administered over two consecutive days (two fractions separated by 6 h on days 1 and 2).

Cell Viability and Clonogenic Survival

Cell viability was determined by trypan blue exclusion at various time points after treatment. Cells were harvested using trypsin, stained with 0.4% trypan blue dye (Sigma T8154), and counted using phase contrast microscopy. For clonogenic survival studies, cells were plated in triplicate in six-well tissue culture dishes at the appropriate density for each condition. After 14 days, the cells were fixed with 100% methanol, air-dried, and stained with 0.1% crystal violet (Sigma C3886). For computing the survival fraction, groups of 50 or more cells were counted as colonies. Data were normalized relative to untreated controls, which were taken as 100% survival.

Terminal Deoxynucleotidyl Transferase-Mediated dUTP Nick End Labeling Assay for Apoptosis

The method of Gavrieli et al. [52] was used as an independent assessment of apoptotic cell death in combined cytopins containing both adherent and nonadherent cells. Cells were fixed, and the fragmented DNA in cells undergoing apoptosis was detected using the In Situ Cell Death Detection kit (Roche 11373242910, 03333566001), where strand breaks are end labeled with fluorescein-dUTP by the enzyme terminal transferase. Cells were then fixed to

glass slides using DAPI-containing Vectashield mounting medium (Sigma D9542). Pictures were taken using an Olympus inverted fluorescence microscope. All images presented are at the same magnification.

Western Blot Analysis

After the indicated treatments, cells were washed in phosphate-buffered saline (PBS) and lysed using 500–1,000 μL M-PER mammalian protein extraction reagent (Thermo Scientific #78501) containing protease and phosphatase inhibitors for 5 min on a shaker. Protein concentrations were determined by the Lowry method, and equal aliquots of protein (40 μg) were separated using 12% SDS-PAGE. Proteins were transferred onto a nitrocellulose membrane and using LI-COR blocking buffer. Membranes were immunoblotted with respective antibodies and then incubated with respective LI-COR secondary antibodies. Proteins were visualized using the LI-COR imaging system. Primary antibodies used were anti-p62 (SQSTM1–Santa Cruz sc-28359), anti-ATG5 (APG5–Biosensis R-111-100), anti-ATG7 APG7–Santa Cruz sc-33211, anti- β actin (Santa Cruz sc-47778), anti α -tubulin (Santa Cruz sc-5286), anti-caspase 3 (Cell Signaling 9665), and anti-PARP (Cell signaling 46D11). All primary antibodies presented were used at a 1:1,000 dilution.

Detection and Quantification of Autophagic Cells by Staining with Acridine Orange

As a marker of autophagy, the volume of the cellular acidic compartment was visualized by AO staining [18]. Cells were seeded in six-well tissue culture dishes and treated as described above for the cell viability study. Seventy-two hours following initial treatment, cells were incubated with medium containing 1 $\mu\text{g}/\text{mL}$ AO (Invitrogen A3568) for 15 min; the AO was then removed, cells were washed once with PBS, fresh media was added, and fluorescent micrographs were taken using an Olympus inverted fluorescence microscope. All images presented are at the same magnification. The number of cells with increased AVO was determined by flow cytometry. Cells were trypsinized, harvested, and analyzed by BD FACSCanto II using BD FACSDiva software. A minimum of 10,000 cells within the gated region were analyzed.

Detection of Autophagic Cells by Staining with Monodansylcadaverine

The autofluorescent agent monodansylcadaverine (Sigma Chemical) was used as a specific autophagolysosome marker [34]. Cells were seeded in six-well tissue culture dishes and treated as described above for the cell viability study. Seventy-two hours following initial treatment, cells were incubated

with medium containing 1 $\mu\text{g}/\text{mL}$ MDC for 15 min; the MDC was then removed, cells were washed once with PBS, fresh media was added, and fluorescent micrographs were taken using an Olympus inverted fluorescence microscope. Again, all images presented are at the same magnification.

Cell Cycle Analysis by Propidium Iodide Staining

For the cell cycle analysis, tumor cells treated as described above were trypsinized, fixed with 70% ethanol, and stained with propidium iodide 72 h posttreatment. Protocol was adapted from Darzynkiewicz et al. [53]. A minimum of 20,000 cells/events were analyzed.

FACS Analysis for Annexin V- and Propidium Iodide-Positive Cells to Monitor Apoptosis and Necrosis

For the FACS analysis, cells treated as described above were collected and labeled fluorescently for detection of apoptotic and necrotic cells by adding 500 μL of binding buffer, 5 μL of annexin V-FITC, and 5 μL of propidium iodide to each sample. Samples were mixed gently and incubated at room temperature in the dark for 15 min. The number of cells with increased annexin/PI staining was determined by flow cytometry and analyzed by BD FACSCanto II using BD FACSDiva software. A minimum of 10,000 cells within the gated region were analyzed.

Transmission Electron Microscopy

TEM services, including sample fixation, embedding, ultramicrotomy, and staining, were provided by the VCU Department of Anatomy and Neurobiology Microscopy Facility. Sections were imaged via Jeol JEM-1230 transmission electron microscope equipped with a Gatan UltraScan 4000SP 4 K \times 4 K CCD camera. The magnification of each image is indicated by the scale bar at the bottom of the micrograph.

Cytochemical Detection of β -Galactosidase Staining

β -galactosidase-positive cells were detected by the method of Dimri et al. [54]. Briefly, the monolayers of cells were washed two times with PBS and then fixed with 2% formaldehyde 1 0.2% glutaraldehyde (prepared in PBS) for 5 min. The cells were then washed again two times with PBS. After the last wash, staining solution was added [1 mg/ml 5-bromo-4-chloro-3-indolyl- β -D-galactoside (X-gal) in dimethylformamide (20 mg/mL stock), 40 mM citric acid/sodium phosphate, pH 6.0, 5 mM potassium ferrocyanide, 5 mM potassium ferricyanide, 150 mM NaCl, 2 mM MgCl_2], and the cells were incubated at 37°C for 24 h. After incubation, the cells were washed two times with PBS and visualized using an Olympus inverted microscope.

FACS Analysis of β -Galactosidase Activity

Cells were treated as described above and analyzed using fluorescent β -galactosidase activity marker C_{12}FDG . The protocol was adapted from Debacq-Chainiaux et al. [39]

RFP-LC3 Redistribution

The MCF7 RFP-LC3 construct was a generous gift from Dr. Keith Miskimins. ZR-75-1 cells were stably transfected with RFP-LC3 using the standard effectene (Qiagen) protocol. Cells were treated as described above and visualized using a Leica confocal laser scanning microscope. Cells were counterstained with DAPI to visualize. Five fields were counted for each treated condition to determine the average number of LC3 puncta per cell.

Statistical Analysis

Statistical differences were determined using StatView statistical software. The data were expressed as the means \pm SE (as standard error of the mean). Comparisons were made using a one-way ANOVA followed by Tukey–Kramer post hoc test. P values ≤ 0.05 were taken as statistically significant.

Acknowledgments Electron and confocal microscopy was performed at the VCU Department of Anatomy and Neurobiology Microscopy Facility, supported, in part, with funding from the NIH-NINDS Center core grant 5P30NS047463. Annexin V/PI staining, β -galactosidase activity, and PI staining for cell cycle analysis and quantification of acridine orange staining were conducted using the VCU Flow Cytometry and Imaging Shared Resource Facility and supported in part by Flow Cytometry Core grant, NIH Grant P30CA16059.

Conflict of Interest There are no conflicts of interest.

Funding Sources Ms. Eden Wilson was supported in part by Award Number F31CA144812 from the National Cancer Institute, American Institute for Cancer Research, grant number 06A058. W. A. Maltese was supported by the U.S. Department of Defense, grant number W81XWH-04-1-0493 and the National Institutes of Health, grant number R01 CA115495.

References

1. Chen DJ, Nirodi CS (2007) The epidermal growth factor receptor: a role in repair of radiation-induced DNA damage. *Clin Cancer Res* 13:6555–6560
2. Spitz DR, Azzam EI, Li JJ et al (2004) Metabolic oxidation/reduction reactions and cellular responses to ionizing radiation: a unifying concept in stress response biology. *Cancer Metastasis Rev* 23:311–322
3. Dent P, Yacoub A, Contessa J et al (2003) Stress and radiation-induced activation of multiple intracellular signaling pathways. *Radiat Res* 159:283–300

4. Sundaram S, Gewirtz DA (1999) The vitamin D3 analog EB 1089 enhances the response of human breast tumor cells to radiation. *Radiat Res* 152:479–486
5. Demasters G, Di X, Newsham I et al (2006) Potentiation of radiation sensitivity in breast tumor cells by the vitamin D3 analogue, EB 1089, through promotion of autophagy and interference with proliferative recovery. *Mol Cancer Ther* 5:2786–2797
6. Light BW, Yu WD, McElwain MC et al (1997) Potentiation of cisplatin antitumor activity using a vitamin D analogue in a murine squamous cell carcinoma model system. *Cancer Res* 57:3759–3764
7. Ravid A, Rocker D, Machlenkin A et al (1999) 1,25-Dihydroxyvitamin D3 enhances the susceptibility of breast cancer cells to doxorubicin-induced oxidative damage. *Cancer Res* 59:862–867
8. Hershberger PA, Yu WD, Modzelewski RA et al (2001) Calcitriol (1,25-dihydroxycholecalciferol) enhances paclitaxel antitumor activity in vitro and in vivo and accelerates paclitaxel-induced apoptosis. *Clin Cancer Res* 7:1043–1051
9. Chaudhry M, Sundaram S, Gennings C et al (2001) The vitamin D3 analog, ILX-23-7553, enhances the response to adriamycin and irradiation in MCF-7 breast tumor cells. *Cancer Chemother Pharmacol* 47:429–436
10. Chen N, Karantzis-Wadsworth V (2009) Role and regulation of autophagy in cancer. *Biochim Biophys Acta* 1793:1516–1523
11. Shintani T, Klionsky DJ (2004) Autophagy in health and disease: a double-edged sword. *Science* 306:990–995
12. Ito H, Daido S, Kanzawa T et al (2005) Radiation-induced autophagy is associated with LC3 and its inhibition sensitizes malignant glioma cells. *Int J Oncol* 26:1401–1410
13. Fung C, Lock R, Gao S et al (2008) Induction of autophagy during extracellular matrix detachment promotes cell survival. *Mol Biol Cell* 19:797–806
14. Wu YT, Tan HL, Huang Q et al (2008) Autophagy plays a protective role during zVAD-induced necrotic cell death. *Autophagy* 4:457–466
15. Maiuri MC, Zalckvar E, Kimchi A et al (2007) Self-eating and self-killing: crosstalk between autophagy and apoptosis. *Nat Rev Mol Cell Biol* 8:741–752
16. Gorka M, Daniewski WM, Gajkowska B et al (2005) Autophagy is the dominant type of programmed cell death in breast cancer MCF-7 cells exposed to AGS 115 and EFDAC, new sesquiterpene analogs of paclitaxel. *Anticancer Drugs* 16:777–788
17. Oh SH, Kim YS, Lim SC et al (2008) Dihydrocapsaicin (DHC), a saturated structural analog of capsaicin, induces autophagy in human cancer cells in a catalase-regulated manner. *Autophagy* 4:1009–1019
18. Paglin S, Hollister T, Delohery T et al (2001) A novel response of cancer cells to radiation involves autophagy and formation of acidic vesicles. *Cancer Res* 61:439–444
19. Gozuacik D, Kimchi A (2007) Autophagy and cell death. *Curr Top Dev Biol* 78:217–245
20. Gewirtz DA, Hilliker ML, Wilson EN (2009) Promotion of autophagy as a mechanism for radiation sensitization of breast tumor cells. *Radiother Oncol* 92:323–328
21. Livesey KM, Tang D, Zeh HJ et al (2009) Autophagy inhibition in combination cancer treatment. *Curr Opin Invest Drugs* 10:1269–1279
22. Lomonaco SL, Finnis S, Xiang C et al (2009) The induction of autophagy by gamma-radiation contributes to the radioresistance of glioma stem cells. *Int J Cancer* 125:717–722
23. Apel A, Herr I, Schwarz H et al (2008) Blocked autophagy sensitizes resistant carcinoma cells to radiation therapy. *Cancer Res* 68:1485–1494
24. Kim KW, Mutter RW, Cao C et al (2006) Autophagy for cancer therapy through inhibition of pro-apoptotic proteins and mammalian target of rapamycin signaling. *J Biol Chem* 281:36883–36890
25. Cao C, Subhawong T, Albert JM et al (2006) Inhibition of mammalian target of rapamycin or apoptotic pathway induces autophagy and radiosensitizes PTEN null prostate cancer cells. *Cancer Res* 66:10040–10047
26. Peng PL, Kuo WH, Tseng HC et al (2008) Synergistic tumor-killing effect of radiation and berberine combined treatment in lung cancer: the contribution of autophagic cell death. *Int J Radiat Oncol Biol Phys* 70:529–542
27. Shen HM, Codogno P (2011) Autophagic cell death: Loch Ness monster or endangered species? *Autophagy* 7:457–465
28. Ingraham BA, Bragdon B, Nohe A (2008) Molecular basis of the potential of vitamin D to prevent cancer. *Curr Med Res Opin* 24:139–149
29. Wu G, Fan RS, Li W et al (1997) Modulation of cell cycle control by vitamin D3 and its analogue, EB1089, in human breast cancer cells. *Oncogene* 15:1555–1563
30. Kwong J, Kulbe H, Wong D et al (2009) An antagonist of the chemokine receptor CXCR4 induces mitotic catastrophe in ovarian cancer cells. *Mol Cancer Ther* 8:1893–1905
31. Portugal J, Mansilla S, Bataller M (2010) Mechanisms of drug-induced mitotic catastrophe in cancer cells. *Curr Pharm Des* 16:69–78
32. Pyo JO, Jang MH, Kwon YK et al (2005) Essential roles of Atg5 and FADD in autophagic cell death: dissection of autophagic cell death into vacuole formation and cell death. *J Biol Chem* 280:20722–20729
33. Eskelinen EL, Saftig P (2009) Autophagy: a lysosomal degradation pathway with a central role in health and disease. *Biochim Biophys Acta* 1793:664–673
34. Zakeri Z, Melendez A, Lockshin RA (2008) Detection of autophagy in cell death. *Methods Enzymol* 442:289–306
35. Kirisako T, Ichimura Y, Okada H et al (2000) The reversible modification regulates the membrane-binding state of Apg8/Aut7 essential for autophagy and the cytoplasm to vacuole targeting pathway. *J Cell Biol* 151:263–276
36. Pankiv S, Clausen TH, Lamark T et al (2007) p62/SQSTM1 binds directly to Atg8/LC3 to facilitate degradation of ubiquitinated protein aggregates by autophagy. *J Biol Chem* 282:24131–24145
37. Larsen KB, Lamark T, Overvatn A et al (2010) A reporter cell system to monitor autophagy based on p62/SQSTM1. *Autophagy* 6:784–793
38. Shvets E, Fass E, Scherz-Shouval R et al (2008) The N-terminus and Phe52 residue of LC3 recruit p62/SQSTM1 into autophagosomes. *J Cell Sci* 121:2685–2695
39. Debaqç-Chainiaux F, Erusalimsky JD, Campisi J et al (2009) Protocols to detect senescence-associated beta-galactosidase (SA-beta-gal) activity, a biomarker of senescent cells in culture and in vivo. *Nat Protoc* 4:1798–1806
40. Shacka JJ, Klocke BJ, Roth KA (2006) Autophagy, bafilomycin and cell death: the “a-B-Cs” of plecomacrolide-induced neuroprotection. *Autophagy* 2:228–230
41. Carew JS, Medina EC, Esquivel JA 2nd et al (2010) Autophagy inhibition enhances vorinostat-induced apoptosis via ubiquitinated protein accumulation. *J Cell Mol Med* 14:2448–2459
42. Klionsky DJ (2005) The molecular machinery of autophagy: unanswered questions. *J Cell Sci* 118:7–18
43. Jones KR, Elmore LW, Jackson-Cook C et al (2005) p53-Dependent accelerated senescence induced by ionizing radiation in breast tumour cells. *Int J Radiat Biol* 81:445–458
44. Mirzayans R, Scott A, Cameron M et al (2005) Induction of accelerated senescence by gamma radiation in human solid tumor-derived cell lines expressing wild-type TP53. *Radiat Res* 163:53–62
45. Botti J, Djavaheri-Mergny M, Pilatte Y et al (2006) Autophagy signaling and the cogwheels of cancer. *Autophagy* 2:67–73

46. Hoyer-Hansen M, Jaattela M (2007) Connecting endoplasmic reticulum stress to autophagy by unfolded protein response and calcium. *Cell Death Differ* 14:1576–1582
47. Qin L, Wang Z, Tao L et al (2010) ER stress negatively regulates AKT/TSC/mTOR pathway to enhance autophagy. *Autophagy* 6:239–247
48. Kim KW, Moretti L, Mitchell LR et al (2010) Endoplasmic reticulum stress mediates radiation-induced autophagy by perkeIF2alpha in caspase-3/7-deficient cells. *Oncogene* 29:3241–3251
49. Zhang Y, Zhang J, Studzinski GP (2006) AKT pathway is activated by 1, 25-dihydroxyvitamin D3 and participates in its anti-apoptotic effect and cell cycle control in differentiating HL60 cells. *Cell Cycle* 5:447–451
50. Lisse TS, Hewison M (2011) Vitamin D: a new player in the world of mTOR signaling. *Cell Cycle* 10:1888–1889
51. Crighton D, Wilkinson S, O'Prey J et al (2006) DRAM, a p53-induced modulator of autophagy, is critical for apoptosis. *Cell* 126:121–134
52. Gavrieli Y, Sherman Y, Ben-Sasson SA (1992) Identification of programmed cell death in situ via specific labeling of nuclear DNA fragmentation. *J Cell Biol* 119:493–501
53. Darzynkiewicz, Z, Li X, Gong J (1994) PI flow for apoptosis. *Methods in Cell Biology* 41:26–29
54. Dimri GP, Lee X, Basile G et al (1995) A biomarker that identifies senescent human cells in culture and in aging skin in vivo. *Proc Natl Acad Sci USA* 92:9363–9367